DOI: 10.24874/ti.1579.11.23.01

Tribology in Industry

www.tribology.rs

RESEARCH

Wheel Squeal Mitigation Under Water Lubrication

Václav Navrátil[a,*], Radovan Galas[a], Milan Klapka[a], Daniel Kvarda[a], Milan Omasta[a]

[a]*Faculty of Mechanical Engineering, Brno University of Technology, Technicka 2896/2, 616 69 Brno, Czechia.*

Keywords:

Wheel squeal noise
Noise mitigation
Friction management
Water lubrication
Wheel-rail tribology

* Corresponding author:

Václav Navrátil
E-mail: Vaclav.Navratil@vutbr.cz

Received: 13 November 2023
Revised: 14 December 2023
Accepted: 26 January 2024

A B S T R A C T

This study investigates the potential of applying water to the wheel-rail contact to reduce squealing noise. For this purpose, a twin-disc device with a single tram wheel and real wheel suspension stiffnesses was developed. Three types of tests were performed. During the tests, adhesion coefficient, sound pressure level and wheel axial vibration were measured. The tests under dry conditions were carried out to describe the frequency spectrum of wheel vibration and to establish reference values for further measurements. The tests under wet conditions were carried out to investigate the ability of water to reduce adhesion and noise. Finally, tests with varying amounts of water in contact were carried out because of the low adhesion risk. The experimental results showed that the twin-disc device was able to reproduce both the adhesion and noise properties of the contact. Tests with different amounts of water showed that the application of water can be a promising way to reduce squealing noise from wheel-rail contact.

1. INTRODUCTION

One of the most unpleasant downsides of railway transport is the curve squealing noise that occurs when rolling stock negotiates a sharp curve. This is mainly due to frictional instabilities in the wheel-rail contact [1] which can occur in several ways [2]. Lateral slip, or creepage, of the wheel tread on the top of the rail plays an important role. This noise, known as a top-of-rail squeal, has a strong tonal character and is very loud, usually exceeding 90 dB [3]. It typically occurs in the 400 – 5000 Hz frequency range [4,5]. Recently, the longitudinal slip has also been shown to influence the occurrence of top-of-rail squeal [6], with the noise occurring in the 3.5 – 6 kHz frequency band [7]. Frictional instabilities can also arise from the interaction of the wheel flange with the gauge face of the rail [3]. Such noise is called flanging noise and is present at higher frequencies over a wide band of 5 – 10 kHz [8,9]. Both types of squeal occur in a largely random, chaotic manner [10–12], and this is mainly due to the large number of parameters that influence the noise generation - e.g. operating parameters such as rolling speed or angle of attack [13], railway track dynamics [14,15], longitudinal creepage [7], etc.

Curve squeal noise is very annoying in densely populated areas, where squealing noise can, according to Müller and Oertli [16], affect up to 1,000 inhabitants within 250 m of the noise source. For this reason, it is important to reduce noise, which can be done in several ways: by passive [17–19] or active vibration control [20,21], or by adjusting the frictional properties

of the wheel-rail contact [22,23]. With wheel vibration damping, the sound pressure level can be reduced by up to 15 dB [24], but this solution is limited by the narrow frequency band to which the damping is tuned. Active wheel vibration control is a new approach that involves mounting actuators on the wheel that damp frequencies based on signals from piezoelectric sensors. This method has been shown to be effective in reducing squeal noise by up to 12 dB in the near field [20], but the system has not yet been used in real-world applications.

Modification of the contact friction properties is possible through the application of various products to the top of the rail head. Top-of-rail (TOR) products include water-based friction modifiers and oil-based TOR lubricants. These products allow the positive trend of the traction curve and the adhesion coefficient to be maintained at an intermediate level. When used on real tracks, sound pressure levels can be reduced by up to 12 dB [8,25]. Recently it has been shown that the application of water to the wheel-rail contact can lead to lower wear [26–28] and noise [29] in addition to reduced adhesion. Several authors show that water can reduce the coefficient of adhesion at levels between 0.2 – 0.45 [30–33] depending on quantity and temperature, or velocity. Water spraying could represent a simple, cheap, and environmentally friendly option for wheel-rail interface lubrication. However, research to date has mainly been carried out on scaled twin discs without a focus on noise reduction, so further research is needed under conditions that more closely resemble real contact.

As it is difficult to control experiments on the real track, test rigs are set up for laboratory research. Naeimi [34] compiled an overview of different approaches and designs but in general, it can be said that due to the ease of slip control and compact dimensions, the twin disc concept is the most common approach to study a single wheel-rail contact. Hsu et al. [4] developed a device which was used to study the adhesion-noise relationship and to validate theoretical models. A similar device was developed at TNO-TPD Delft and used to study the effect of longitudinal creepage together with lateral creepage [35,36]. Another device was built at the University of Queensland. The primary motivation for building the device was to study corrugation formation and wear [37], but later, it was used by Meehan and Liu [13,38,39] to experimentally validate the developed simulation models and predictions of squealing noise generation. The device was further modified and Liu [40] used it to investigate the effect of contact angle on noise generation.

This study aims to investigate the potential reduction of wheel squeal noise through the application of water into the wheel-rail contact area. For this purpose, the twin-disc test rig with a real tram wheel was designed and used, see Fig. 1. During the design process, emphasis was placed on maintaining the realistic stiffness of the wheel fit in the tram chassis. Detailed information regarding the design of this device can be found in the paper [41]. The analysis of the effects of water application on wheel-rail interaction is intended to contribute to the knowledge of noise reduction techniques and a better understanding of the factors influencing wheel squeal.

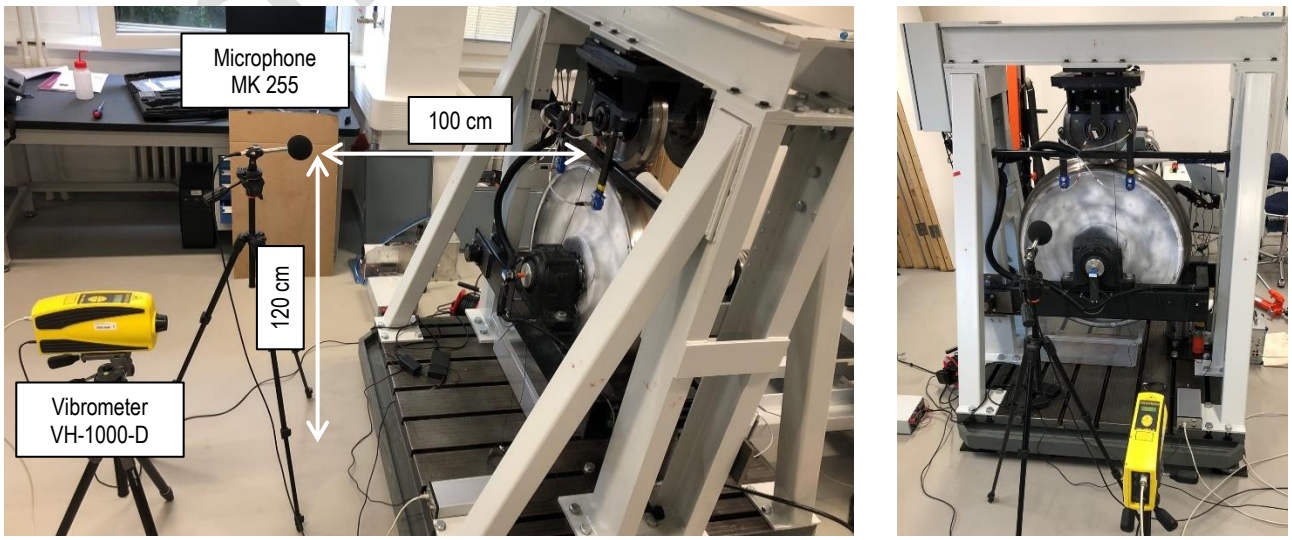

Fig. 1. Experimental twin-disc device.

2. MATERIAL AND METHODS

2. 1 Experimental methods

The main parts of the device in Fig. 1 are tram wheel with ORE S 1002 profile with a diameter of 800 mm and 320 mm diameter rail disc. The disc is made of C55E steel. This material does not correspond to the actual rail material but was chosen for higher wear resistance and longer maintenance of stable conditions during testing. The wheel is mounted on a structure that is pivotally attached to the main frame and the contact loading is thus realized by a lever using a hydraulic cylinder and a compression coil spring. The disc is mounted on a support that allows the disc to be rotated to change the angle of attack, and the disc to be moved to change the lateral position of the disc thanks to a pair of linear guideways. The 11 kW AC electric motor with a gearbox, which drives the wheel, is mounted on an independent frame. The test rig was designed with the required dynamic characteristics in mind. To achieve the required dynamic properties of the wheel and suspension disc, the stiffness of certain elements in the support frame was optimised. By optimising the stiffness of the bridging beams at the top of the rig, the normal stiffness of the rail disc was determined. This, together with the lateral stiffness of the positioning system, also influences the lateral stiffness of the rail disc. The normal stiffness of the wheel was determined by selecting a compression spring in the loading mechanism with the appropriate stiffness. The lateral stiffness of the wheel corresponds to the stiffness of the beams that make up the wheel lever. The stiffness of the elements was designed using FEM software and analytical calculations. The parameters of the twin-disc device can be found in Table 1. A more detailed description of the device can be found in the paper [41].

An integral part of the equipment is the measuring system. To evaluate the lateral adhesion coefficient, it is necessary to measure the load and lateral force. Two load cells are used for this purpose. The first one is part of the load mechanism and reads the force in the range of 0 – 10 kN. The second is mounted in the disc support and measures the lateral force in the range of 0 – 5 kN. The sampling frequency of 500 Hz for the force measurements is set. Lateral adhesion coefficient can be calculated according to Hsu [4]:

$$\mu = 0{,}5196\frac{F_2}{F_1} \quad (1)$$

where F_2 is the lateral force and F_1 is the load force.

Table 1. Parameters of twin-disc device.

Parameter	Value	Unit
Outer dimensions	1340 x 3020 x 1690	mm
Weight	2270	Kg
Wheel diameter	800	mm
Wheel profile	ORE S 1002	-
Rail disc diameter	320	mm
Rail disc profile radius	100	mm
Maximum velocity	4	m/s
Wheel drive torque	1000	Nm
Wheel drive power	11	kW
Ange of attack range	±5	°
Wheel normal suspension	0.172	kN/mm
Wheel lateral suspension	5.21	kN/mm
Rail disc normal suspension	124	kN/mm
Rail disc lateral suspension	6	kN/mm

The numerical coefficient expresses the ratio of the oversteer because the load force is not measured in the axis of contact but at the end of the arm on which the wheel is mounted.

Another important parameter to evaluate is the lateral creepage. According to Meehan and Liu [30], the quasi-static value of lateral creepage equals the angle of attack. Two ultrasonic sensors SICK UM12-1172271 are used to read the position of the disc and the resulting angle of attack can be calculated according to the scheme in Fig. 2 using the equation:

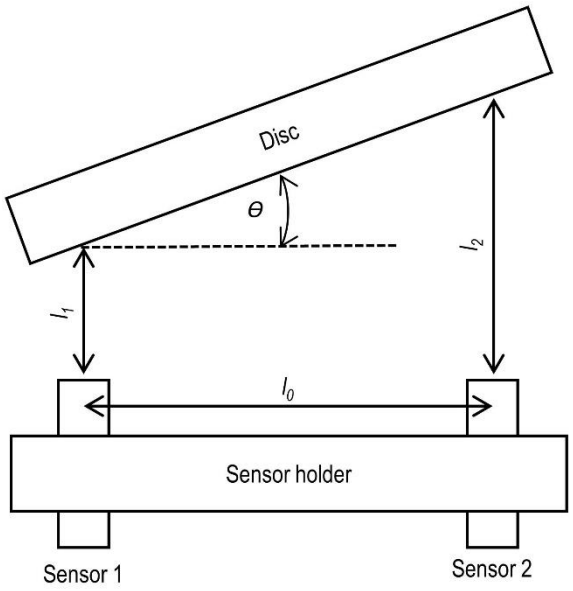

Fig. 2. Angle of attack evaluation scheme.

$$\theta = tan^{-1}\left(\frac{l_2 - l_1}{l_0}\right) \quad (2)$$

where l_1 and l_2 are measured distance to the disc from sensor no. 1 and 2, respectively, l_0 is the distance between sensors, which for the device used is 286 mm. The sampling frequency for distance measurements is set to 500 Hz.

2.2 Noise and vibration measurements

The twin-disc is not equipped with any vibration and noise measuring equipment; therefore, the use of external equipment is necessary. For noise measurements, a Svantek 911 sound meter with MK 255 microphone and SV 12L preamplifier was used to record the noise data. The noise was recorded in the frequency range 20 Hz – 20 kHz and no weighting filter was used. The microphone was placed 100 cm from the wheel-disc contact at contact height (120 cm), see Fig. 1.

To correctly identify the frequencies at which only the wheel emits noise, wheel vibration was also measured. An Ometron VH-1000-D industrial laser Doppler vibrometer connected to Brüel & Kjær PULSE™ data acquisition system was used to measure wheel vibration. The vibration was scanned in the axial direction with the laser aimed at the edge of the wheel tyre. Data was acquired in the frequency range of 20 Hz – 22 kHz. Fast Fourier transform analysis was used to obtain the frequency spectrum of vibration.

2.3 Data validation

Finite Element Method (FEM) modal analysis was carried out using ANSYS to gain a comprehensive understanding of the dynamic behaviour of the wheel. This analysis provided insight into the structural response of the wheel, revealing its natural frequencies, and associated modal shapes. By simulating the vibrational behaviour, we identified critical modes of vibration, such as those that could lead to resonant conditions, and assessed their impact on the wheel's performance.

To ensure the accuracy and reliability of the adhesion values measured in this study, a validation procedure was required. The validation procedure involved a comparison of the measured adhesion data with simulations obtained from the established model developed by de Beer [35], see equation (3):

$$\mu = \begin{cases} \mu_K\left\{\zeta' - \frac{1}{3}\zeta'^2 + \frac{1}{27}\zeta'^3\right\} & \text{for } \zeta' \le 3 \\ \mu_K & \text{for } \zeta' > 3 \end{cases} \quad (3)$$

where μ_K is the realistic friction characteristic defined in [42]as:

$$\mu_K = \mu_0\left\{1 - 0.5e^{-0.138/|\zeta V_0|} - 0.5e^{-6.9/|\zeta V_0|}\right\} \quad (4)$$

where μ_0 is static friction coefficient, V_0 is rolling speed, ζ is nominal lateral creepage calculated according to equation (5):

$$\zeta = \frac{\theta}{\cos\theta_C} \quad (5)$$

using angle of attack θ and contact angle θ_C, ζ' is normalised creepage which can be obtained from equation (6):

$$\zeta' = \frac{\zeta k_\zeta}{N} \quad (6)$$

where k_ζ is the contact parameter and N is the load. Using this validated simulation model, we aimed to confirm the consistency of our experimental results with the expected results based on established theoretical frameworks. This approach not only increases the robustness of our results but also allows us to assess the validity of our measurement techniques and their agreement with theoretical predictions.

2.4 Experimental procedure

Three types of tests were performed in this study. The purpose of tests under dry conditions was to describe the frequency spectrum of wheel vibration and to establish reference values for subsequent comparison with wet contact. The tests were carried out at two speeds, 2 and 4 m/s. The lower speed is the speed at which trams normally travel through the loop and the higher speed is close to the limit at which trams are allowed to travel through the loop. The contact force was chosen to be 1,000 N (≈ 600 MPa) according to Meehan [43]. In the loop, the angle of attack reaches values of around 2° (≈ 35 mrad), so tests were carried out in the range 0 – 35 mrad. The experiments were performed at room temperature (25 °C). In addition to adhesion, sound pressure and vibration levels were also recorded, see sections 2.1 and 2.2. All tests were repeated three times and traction curves for each speed were made from the average of three measurements for each angle of attack. Before each test, the wheel and disc were cleaned with paper towels, acetone and water as in the previous study [29].

The tests under wet conditions were carried out under the same conditions as the tests under dry conditions. Water was continuously applied to the contact at a rate of 5 ml/s for 20 s. Before each test, the wheel and disc were cleaned in the same way as for the tests under dry conditions tests. A traction curve was also constructed in the same way and the sound pressure level and wheel vibration were measured.

The final part of the experiments focused on the effect of the amount of water applied to the wheel-rail contact. The motivation was to see if the amount of water in contact influenced the development of low adhesion (μ < 0.1). The tests were carried out under a uniform setup with a speed of 4 m/s, a contact load of 1,000 N, an angle of attack of 20 mrad, and at room temperature. Amounts of 1, 2, 5 and 10 ml were used for the experiments. Each test was repeated three times. Three parameters were monitored during the tests: the change in adhesion ($\Delta\mu$), the change in sound pressure level (ΔSPL) and the retentivity (Δt), i.e., the time between the application of water and the achievement of the reference values, see Fig. 3.

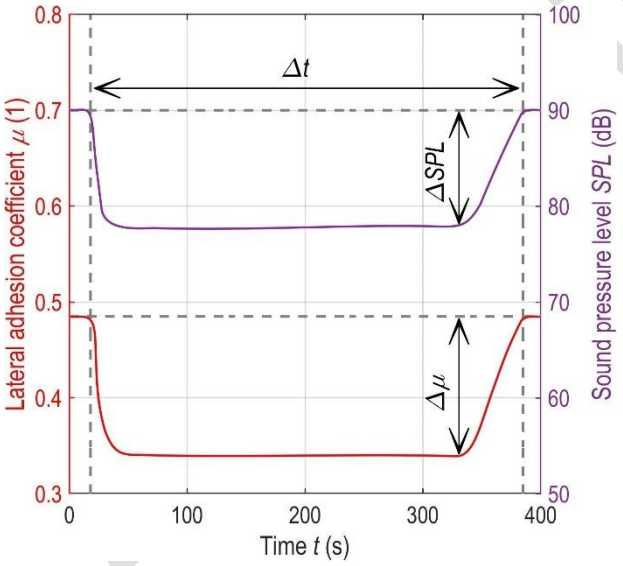

Fig. 3. A typical development of μ and SPL over time.

3. RESULTS AND DISCUSSION

3.1 Modal analysis

The results of the analysis revealed six dominant frequencies in the 0 – 5 kHz range at which wheel oscillations can be expected, see Table 2. The resulting frequencies are similar to those reported by Liu [13] in his paper. The largest differences are at frequencies below 1 kHz, but these are due to the use of a different wheel profile. The agreement with Liu's results for the (3,0) mode, see Fig. 4, is important, as this mode is described by the authors as prone to squeal. The FEM analysis showed that modes exist in pairs, i.e., two modes have identical natural frequencies and modal shapes with phase shift between them, which is the typical feature of an axisymmetric structure [4].

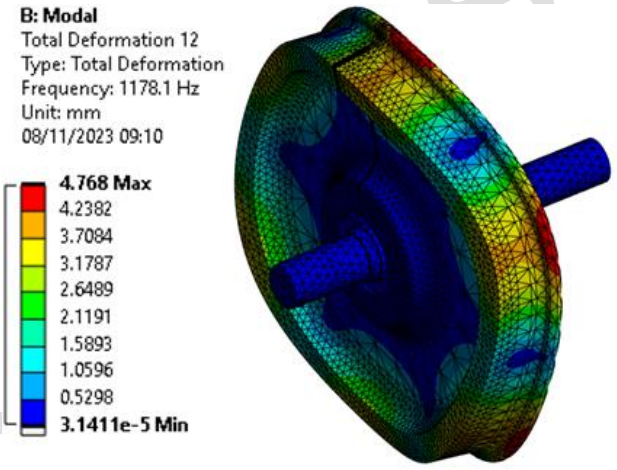

Fig. 4. Visualization of wheel modal shape (3,0) - 1178 Hz.

Table 2 Results of FEM modal analysis.

Dominant frequency (Hz)	Vibration mode (*n*,*m*)	Mode shape
295	(1,0)	
475	(2,0)	
1178	(3,0)	
2013	(4,0)	
3125	(5,0)	
4202	(6,0)	

3.2 Measurements under dry conditions

The results of the experiments under dry conditions in Fig.5 show that the measured adhesion coefficient at the saturation point of the traction curve is around 0.5, which is

expected value [44]. After fitting the data with the simulation model of de Beer [35] with parameter settings according to Meehan [43], it can be concluded that the measured data fit the simulation well. The deviation of the measured data from the simulation is due to a combination of uncertainties in the load and lateral force measurements. According to Hsu [4], uncertainty in the measurement of the adhesion coefficient can be expressed as:

$$\delta\mu = \sqrt{(\delta F_1/F_1)^2 + (\delta F_2/F_2)^2} \quad (7)$$

Both load cells were used to measure with an error of 5 %. Substituting this value into the formula gives an uncertainty in the lateral adhesion coefficient of approximately 7 %. Converted to adhesion coefficient values, an error of ±0.04 can be expected. This band is shown in Fig. 5 by error lines. All results, which are listed in Table A1 in the Supplementary Material, are within this tolerance.

The measured sound pressure levels increased with increasing angle of attack and also with higher rolling velocity, see Table A2 in the Supplementary Material, which was expected given the results of Meehan [13,38]. The frequency composition of the measured noise is shown in Fig. 6. In the figure, peaks can be observed at frequencies that correspond to the simulation, but the signal is significantly affected by noise from other components of the twin-disc device, e.g. the rail disc.

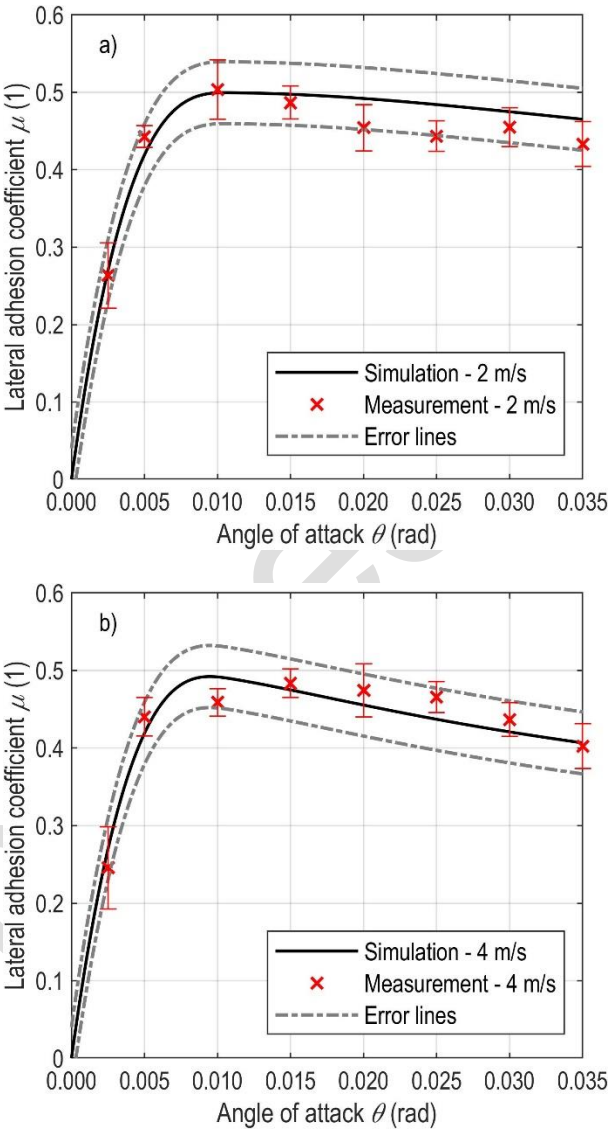

Fig. 5. Results of experiments under dry conditions for speed: (a) 2 m/s, (b) 4 m/s.

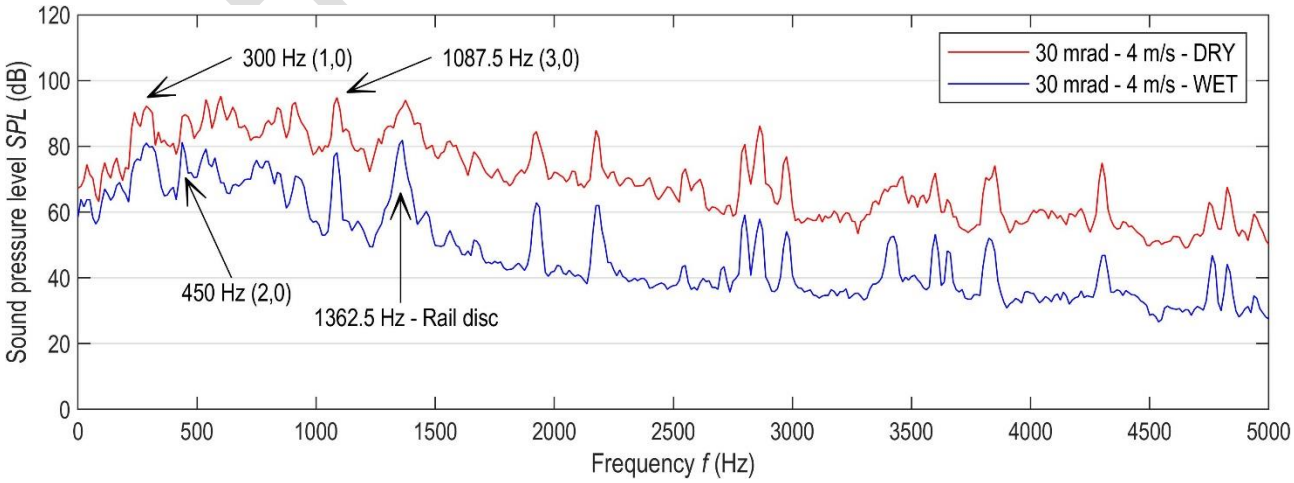

Fig. 6. Frequency composition of measured noise under dry (red) and wet (blue) conditions.

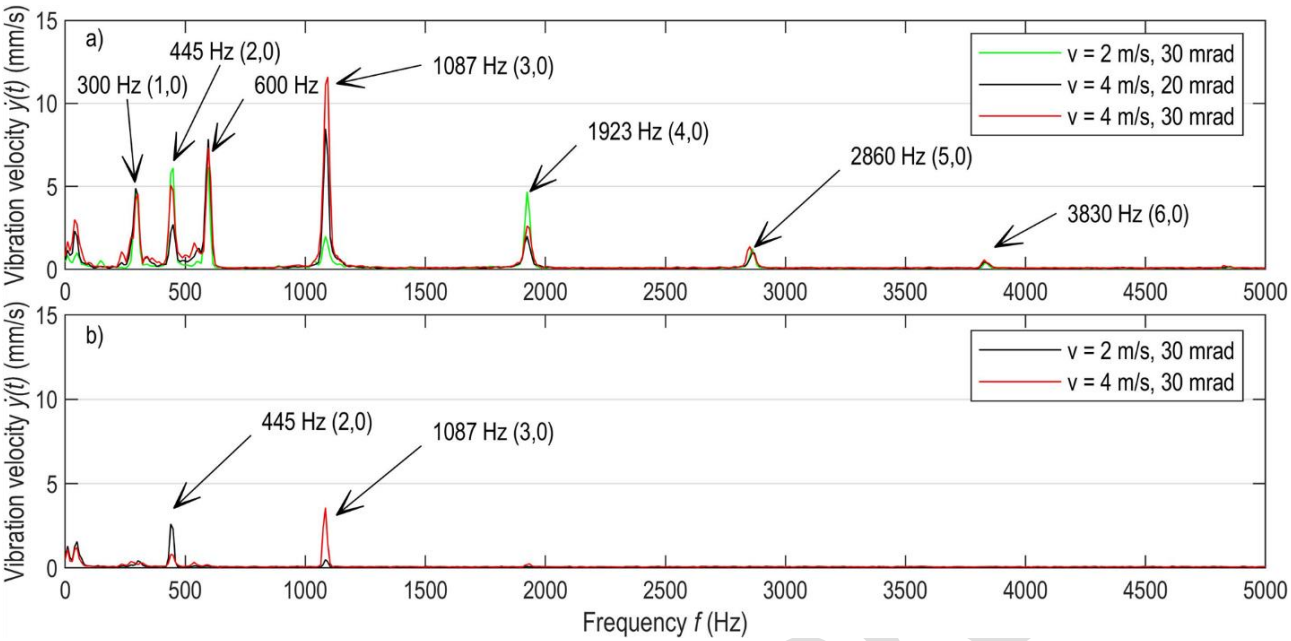

Fig. 7. Frequency composition of measured vibrations in (a) dry contact, and (b) wet contact.

Therefore, the vibration spectrum is more suitable for validating the noise manifestations as it is not as affected by any other component of the twin-disc device as the noise spectrum. The results of the vibration frequency analysis of the measurements under dry conditions are shown in Fig. 7(a) and listed in Tables A3 – A5 in the Supplementary Material. The frequencies of the wheel vibration modes can be identified in the graph, namely 300, 445, 1087, 1923, 2860 and 3830 Hz. These frequencies agree with the results of the modal finite element analysis in ANSYS, although there are minor differences of a few units of Hz for the lower frequencies and low hundreds of Hz for the higher frequencies. This inaccuracy is due to the simplification of the wheel geometry and mounting for the FEM analysis. A frequency of 600 Hz still appears in the frequency spectrum, which does not correspond to the FEM analysis. Control measurements showed that this frequency corresponds to the lateral vibration of the wheel mounting structure. Essentially all the modes identified by FEM analysis appear in the frequency spectrum, but the most dominant vibration mode is at 1100 Hz and is mainly excited at the higher speed of 4 m/s. Meehan and Liu [13,38–40] or Ding [45] also work with this frequency mode in their models. It is important to note that the study is focused on the tram wheel. Different frequency modes are expected for the larger railway wheels used, for example, on freight trains. The results also confirm the findings of Meehan and Liu [13] who state that the vibration velocity amplitude increases with increasing rolling velocity and angle of attack. Interestingly, at lower velocities, the vibration modes at 445 and 1923 Hz are more excited than the mode at 1087 Hz. These findings may lead to the idea of excitation of the vibration modes according to the operating conditions, i.e. which vibration mode becomes dominant depends on what operating conditions prevail. This hypothesis should be the subject of further research.

3.3 Measurements under wet conditions

The results of the tests under wet conditions are shown in Fig. 8 and listed in Table A1 in the Supplementary Material. It can be seen from the graphs that the lateral adhesion coefficient decreases after the application of water by up to 20 % compared to simulation under dry conditions in angle of attack range of 5 – 20 mrad. The values of the lateral adhesion coefficient range from 0.3 to 0.4 for angles of attack of 5 mrad and above, which is within the expected range of 0.2 to 0.45 [31]. The experimental results for both rolling speeds are rather constant after passing the saturation point. After the application of water to the contact, there is probably no increase in contact temperature with increasing slip. Water probably acts as a cooling medium and may prevent the formation of oxide layers that reduce the adhesion coefficient, thus

keeping the trend of the traction curve neutral [46,47]. Therefore, the traction curves in Fig. 8 were obtained by modifying equation (3) according to Shen [48]:

$$\mu = \begin{cases} \mu_0 \left\{ \zeta' - \frac{1}{3}\zeta'^2 + \frac{1}{27}\zeta'^3 \right\} & \text{for } \zeta' \leq 3 \\ \mu_0 & \text{for } \zeta' > 3 \end{cases} \quad (8)$$

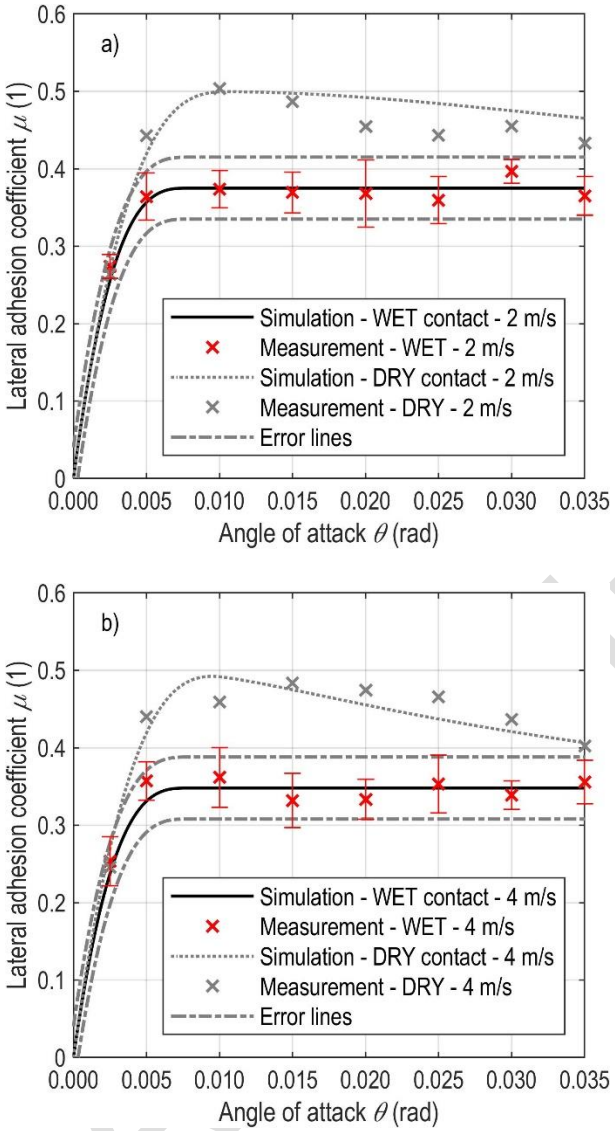

Fig. 8. Results of experiments under wet conditions for speed: (a) 2 m/s, (b) 4 m/s.

To fit the measured data to the simulation curve, it was necessary to determine the value of the static coefficient of friction. This value was estimated using the method of least squares, the aim being to find the smallest deviation of the simulation curve from the data. Using this method, the value of the static coefficient of friction was determined to be 0.375 for rolling speed 2 m/s and 0.348 for 4 m/s. The lateral adhesion coefficient appears to decrease slightly as the rolling speed increases to 4 m/s. This is contrary to the general conclusions drawn by Liu and Meehan in their study [30]. On the other hand, after analyzing their results, it is clear that the increase in the lateral adhesion coefficient is not linear and only occurs at high speeds, up to 25 m/s in the case of the study [30]. It can therefore be assumed that the lateral adhesion coefficient decreases with increasing speed up to a certain speed, after which the trend is reversed. This hypothesis could be the subject of further research.

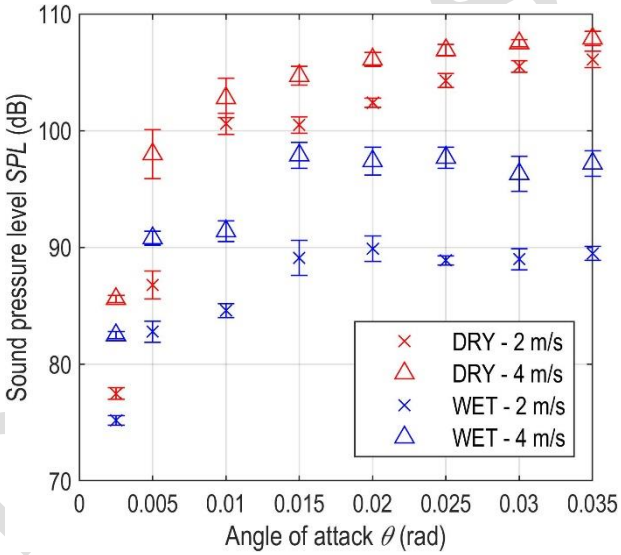

Fig. 9 Evolution of SPL with increasing speed and angle of attack.

Looking at the frequency spectrum of the measured noise in Fig. 6, it can be seen that there is a reduction in noise over a wide range of frequencies. Fig. 9 and Table A2 in the Supplementary Material also show that noise reduction in wet conditions is dependent on rolling speed. At 2 m/s there are reductions of up to 11 – 17 dB beyond the saturation point, while at 4 m/s the reductions are lower, up to 9 – 11 dB. The explanation is that greater dynamic effects at higher rolling speeds lead to an increase in stored acoustic energy and hence a higher overall SPL. The frequency spectrum of the vibration in dry (Fig. 7(a)) and wet (Fig. 7(b)) contact shows that applying water significantly reduces the overall amplitude of the vibration velocity across the entire spectrum, thus reducing the squealing noise. Again, it was observed that at a lower speed of 2 m/s, the 445 Hz frequency is excited. This again raises the idea of excitation of the vibration modes according to the operating conditions. All results are listed in Tables A3 – A5 in the Supplementary Material. The mechanism

by which water reduces noise and vibration in contact is related to the fact that the water can form a lubricating film with the oxides and wear particles in contact similar to the boundary lubrication film that TOR products create [32]. However, as it does not contain all the typical components of a TOR product, it does not reduce adhesion as much as has been observed with TOR products. Such a film is still able to reduce the number of peaks and valleys that interact with each other, thereby reducing the lateral force. This then leads to a reduction in the out-of-plane vibration of the wheel and hence a reduction in the amplitude of sound pressure levels [49].

3.4 Effect of the applied amount of water

The experimental results show that the amount of water applied can affect the adhesion conditions in contact, see Fig. 10. In the case of 1 ml of water applied, there was a large variance in the reduction in adhesion in the tests compared to the other amounts. This may be due to the method of water application, which was from a syringe into the contact area. With such a small amount, even a noticeable deviation from the contact patch may play a role. It is also interesting to note that an amount of 10 ml reduced adhesion the least. This may be related to the fact that in a fully flooded contact, water may wash out debris, which, together with iron oxides, may reduce the resulting adhesion to lower values, as has been observed by other authors [50–52]. The results of the experiments are listed in Table A6 in the Supplementary Material.

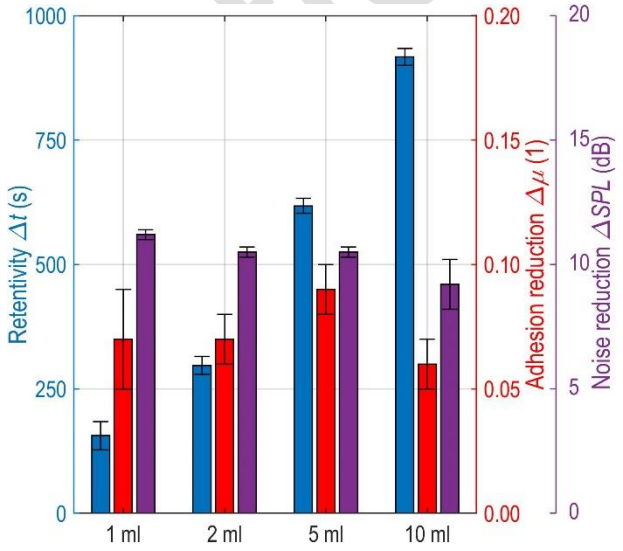

Fig. 10. Comparison of retentivity, adhesion and noise reduction for different amounts of water.

A look at noise reduction shows similar conclusions to the adhesion results. The application of 1, 2 and 5 ml of water resulted in a stable noise reduction of up to 11 – 12 dB. For the 10 ml application, the noise reduction was lower, only around 9 dB. Again, this is attributed to the fact that larger amounts of water are more effective at washing off oxides, which could lead to greater reductions, than smaller amounts of water. A significant difference was observed in the case of the retentivity of water in wheel-rail contact. The retentivity increased significantly with increasing amounts of water applied, which was expected and corresponds with Galas' results [50]. This is because more water takes longer to evaporate from the contact path. In addition, larger volumes of water will also flood the area around the contact, allowing further flooding of the contact and thus increasing the retentivity. When comparing the results, the dependence of retentivity on the amount of water applied appears to be linear.

These data show that water itself could be considered as a solution for reducing wheel squeal noise. An important finding is that the amount of water does not lead to low adhesion that can occur with an incorrect dosage of water-based and oil/grease-based top-of-rail products [49,53–57]. These results are in line with previous work [29]. It can be expected that more frequent applications will be required compared to a water- and oil-based top-of-rail product; on the other hand, the application of clean water represents an environmentally friendly way to achieve similar noise reductions, which are up to 12 dB on a real track [8,25].

3.5 Future study

The next study should focus on the problem of low adhesion. It turns out that the interaction of water with contaminants can lead to the formation of a highly viscous paste that causes this phenomenon [58,59]. This can then cause problems when starting and breaking rolling stock. From an operational safety point of view, this phenomenon should be avoided. The study should be carried out on a twin-disc rig with a real railway wheel to make the contact conditions as close as possible to real track conditions. Also, further research should focus on the idea of excitation of the vibration modes depending on the operating conditions. The

acoustic measurements should be extended to include acoustic emission measurements, which could provide a deeper insight into the coupling of friction film and noise manifestations. If conditions can be found that guarantee noise reduction without risking low adhesion, these conditions should be tested on a real track.

4. CONCLUSIONS

Our research seeks to provide solutions to mitigate wheel squeal noise. One of these solutions may be the application of water to the wheel-rail contact. This solution could lead to an improvement in the overall environmental quality. A newly developed twin-disc device was used to study the effect of water application on squeal noise. The main results of this work are:

- The twin-disc device, designed to simulate as closely as possible the actual wheel-rail contact on a tram track, can produce data that is consistent with current theory and the results of other authors. It can therefore be considered valid.
- The results of the experiments under dry and wet conditions lead to the idea of excitation of the vibration modes depending on the operating conditions, which should be further investigated.
- Applying water to the wheel-rail contact significantly reduces the excitation of the wheel's frequency modes, thereby reducing the squeal noise. At the same time, it does not cause low adhesion problems. The total reduction of emitted noise is up to 9 – 17 dB depending on rolling velocity and angle of attack.
- The amount of water applied does not affect noise reduction and more water does not increase the risk of low adhesion. The only difference observed was an increase in noise and adhesion reduction time as the amount of water applied increased.

Acknowledgement

This research was supported by the Czech Science Foundation (Project No. 20-23482S). The authors would also like to thank the Faculty of Mechanical Engineering at the Brno University of Technology for support within the F22-12 project.

REFERENCES

[1] P.J. Remington, "*Wheel/rail squeal and impact noise: What do we know? What don't we know? Where do we go from here?,"* Journal of Sound and Vibration, vol. 116, pp. 339–353, 1987. doi: 10.1016/S0022-460X(87)81306-8.

[2] D. Alarcao, J.L. Bento Coelho, "*An experimental assessment on the performance of fixed rail lubricators for curve squealing noise mitigation,"* Noise Control Engineering Journal, vol. 61, pp. 567-577, 2013. doi: 10.3397/1/3761050

[3] D. Thompson, "*Curve Squeal Noise,"* in: Railway Noise and Vibration, Elsevier, 2009: pp. 315–342. doi: 10.1016/B978-0-08-0451473.00009 -8.

[4] S.S. Hsu, Z. Huang, S.D. Iwnicki, D.J. Thompson, C.J.C. Jones, G. Xie, P.D. Allen, "*Experimental and theoretical investigation of railway wheel squeal*," Proceedings of the Institution of Mechanical Engineers, Part F: Journal of Rail and Rapid Transit, vol. 221, pp. 59–73, 2007. doi: 10.1243/0954409JRRT85.

[5] J.F. Brunel, P. Dufrénoy, J. Charley, F. Demilly, "*Analysis of the attenuation of railway squeal noise by preloaded rings inserted in wheels,"* Journal of the Acoustical Society of America, vol. 127, pp. 1300 – 1306, 2010. doi: 10.1121/ 1.3298433.

[6] D.J. Fourie, P.J. Gräbe, P.S. Heyns, R.D. Fröhling, "*Experimental characterisation of railway wheel squeal occurring in large-radius curves*," Proceedings of the Institution of Mechanical Engineers, Part F: Journal of Rail and Rapid Transit, vol. 230, pp. 1561–1574, 2016. doi: 10.1177/0954409715605142.

[7] D.J. Fourie, P.J. Gräbe, P.S. Heyns, R.D. Fröhling, "*Frequency domain model for railway wheel squeal resulting from unsteady longitudinal creepage*," Journal of Sound and Vibration, vol. 445, pp. 228–246, 2019. doi: 10.1016/j.jsv. 2018.12.014.

[8] D.T. Eadie, M. Santoro, J. Kalousek, "*Railway noise and the effect of top of rail liquid friction modifiers: Changes in sound and vibration spectral distributions in curves,"* Wear, vol. 258, pp. 1148 – 1155, 2005. doi: 10.1016/j.wear.2004. 03.061.

[9] Y.-K. Luo, L. Zhou, Y.-Q. Ni, "*Towards the understanding of wheel-rail flange squeal: In-situ experiment and genuine 3D profile-enhanced transient modelling,"* Mechanical Systems and Signal Processing, vol. 180, no. 109455, 2022. doi: 10.1016/j.ymssp.2022.109455.

[10] C. Glocker, E. Cataldi-Spinola, R.I. Leine, "*Curve squealing of trains: Measurement, modelling and simulation,"* Journal of Sound and Vibration, vol. 324, pp. 365–386, 2009. doi: 10.1016/j.jsv.2009.01.048.

[11] Z. Yang, Z. Li, "*Numerical modeling of wheel-rail squeal-exciting contact*," International Journal of Mechanical Sciences, vol. 153–154, pp. 490–499, 2019. doi: 10.1016/j.ijmecsci.2019.02. 012.

[12] P.A. Meehan, "*Investigation of chaotic instabilities in railway wheel squeal*," Nonlinear Dynamics, vol. 100, pp. 159–172, 2020. doi: 10.1007/ s11071-020-05493-x.

[13] X. Liu, P.A. Meehan, "*Wheel squeal noise: A simplified model to simulate the effect of rolling speed and angle of attack*," Journal of Sound and Vibration, vol. 338, pp. 184–198, 2015. doi: 10.1016/j.jsv.2014.10.031.

[14] B. Ding, G. Squicciarini, D. Thompson, *"Effect of rail dynamics on curve squeal under constant friction conditions*," Journal of Sound and Vibration, vol. 442, pp. 183–199, 2019. doi: 10.1016/j.jsv.2018.10.027.

[15] V.-V. Lai, O. Chiello, J.-F. Brunel, P. Dufrénoy, "*The critical effect of rail vertical phase response in railway curve squeal generation*," International Journal of Mechanical Sciences, vol. 167, no. 105281, 2020. doi: 10.1016/j.ijmecsci. 2019.105281.

[16] B. Müller, J. Oertli, "*Combating Curve Squeal: Monitoring existing applications*," Journal of Sound and Vibration, vol. 293, pp. 728–734, 2006. doi: 10.1016/j.jsv.2005.12. 005.

[17] J.F. Brunel, P. Dufrénoy, F. Demilly, "*Modelling of squeal noise attenuation of ring damped wheels*," Applied Acoustics, vol. 65, pp. 457–471, 2004. doi: 10.1016/j.apacoust.2003.12. 003.

[18] J. Han, Z. Wen, R. Wang, D. Wang, X. Xiao, G. Zhao, X. Jin, "*Experimental study on vibration and sound radiation reduction of the web-mounted noise shielding and vibration damping wheel*," Noise Control Engineering Journal, vol. 62, pp. 110 – 122, 2014. doi: 10.3397/1/ 376211.

[19] Y.-S. Yun, J.-C. Kim, "*Reducing Curve Squeal Noise Using Composite Materials Based on Experimental Investigation*," International Journal of Precision Engineering and Manufacturing, vol. 22, pp. 1573–1582, 2021. doi: 10. 1007/s12541-021-00540-y.

[20] S.R. Marjani, D. Younesian, "*Active Vibration Control for the Mitigation of Wheel Squeal Noise Based on a Fuzzy Self-Tuning PID Controller*," Shock and Vibration, vol. 2022, pp. 1–17, 2022. doi: 10.1155/2022/3978230.

[21] W. Kropp, J. Theyssen, A. Pieringer, "*The application of dither to mitigate curve squeal*," Journal of Sound and Vibration, vol. 514, no. 116433, 2021. doi: 10.1016/j.jsv.2021.116433

[22] R. Stock, L. Stanlake, C. Hardwick, M. Yu, D. Eadie, R. Lewis, "*Material concepts for top of rail friction management – Classification, characterisation and application*," Wear, vol. 366–367, pp. 225 – 232, 2016. doi: 10.1016/j.wear. 2016.05.028.

[23] D.T. Eadie, M. Santoro, W. Powell, "*Local control of noise and vibration with KELTRACK™ friction modifier and Protector® trackside application: An integrated solution*," Journal of Sound and Vibration, vol. 267, pp. 761–772, 2003. doi: 10.1016/S0022-460X(03) 00739-9.

[24] J.T. Nelson, "*Wheel/Rail Noise Control Manual*." Transit Cooperative Research Program (TCRP) Report 23, published by Transportation Research Board, Washington, 1997.

[25] D.T. Eadie, M. Santoro, *"Top-of-rail friction control for curve noise mitigation and corrugation rate reduction*," Journal of Sound and Vibration, vol. 293, pp. 747 – 757, 2006. doi: 10.1016/ j.jsv.2005.12.007.

[26] C. Hardwick, R. Lewis, D.T. Eadie, "*Wheel and rail wear—Understanding the effects of water and grease*," Wear, vol. 314, pp. 198–204, 2014. doi: 10.1016/j.wear.2013.11.020.

[27] W.J. Wang, R. Lewis, B. Yang, L.C. Guo, Q.Y. Liu, M.H. Zhu, "*Wear and damage transitions of wheel and rail materials under various contact conditions*," Wear, vol. 362–363, pp. 146–152, 2016. doi: 10.1016/j.wear.2016. 05.021.

[28] H. Lee, "*The effect of water lubricant on reducing the generation of airborne wear particles from wheel–rail contacts under various train velocities*," Tribology International, vol. 150, no. 106393, 2020. doi: 10.1016/j.triboint.2020. 106393.

[29] V. Navrátil, R. Galas, M. Klapka, D. Kvarda, M. Omasta, L. Shi, H. Ding, W.-J. Wang, I. Krupka, M. Hartl, "*Wheel Squeal Noise in Rail Transport: The Effect of Friction Modifier Composition*," Tribology in Industry, vol. 44, pp. 361–373, 2022. doi: 10.24874/ti.1211.11.21.02.

[30] X. Liu, C. Xiao, P.A. Meehan, *"The effect of rolling speed on lateral adhesion at wheel/rail interface under dry and wet condition*," Wear, vol. 438–439, no. 203073, 2019. doi: 10.1016/j. wear.2019.203073.

[31] H. Chen, M. Ishida, A. Namura, K.-S. Baek, T. Nakahara, B. Leban, M. Pau, "*Estimation of wheel/rail adhesion coefficient under wet condition with measured boundary friction coefficient and real contact area*," Wear, vol. 271, pp. 32–39, 2011. doi: 10.1016/j.wear.20 10.10.022.

[32] B. White, R. Lewis, *"Simulation and understanding the wet-rail phenomenon using twin disc testing,"* Tribology International, vol. 136, pp. 475–486, 2019. doi: 10.1016/j.triboint.2019. 03.067.

[33] H. Chen, S. Fukagai, Y. Sone, T. Ban, A. Namura, "*Assessment of lubricant applied to wheel/rail interface in curves,"* Wear, vol. 314, pp. 228–235, 2014. doi: 10.1016/j.wear.2013. 12.006.

[34] M. Naeimi, Z. Li, R.H. Petrov, J. Sietsma, R. Dollevoet, "*Development of a New Downscale Setup for Wheel-Rail Contact Experiments under Impact Loading Conditions,"* Experimental Techniques, vol. 42, 2018. doi: 10.1007/ s40799-017-0216-z.

[35] F.G. De Beer, M.H.A. Janssens, P.P. Kooijman, "*Squeal noise of rail-bound vehicles influenced by lateral contact position,"* Journal of Sound and Vibration, vol. 267, pp. 497–507, 2003. doi: 10.1016/S0022-460X(03) 00710-7.

[36] A.D. Monk-Steel, D.J. Thompson, F.G. de Beer, M.H.A. Janssens, *"An investigation into the influence of longitudinal creepage on railway squeal noise due to lateral creepage,"* Journal of Sound and Vibration, vol. 293, pp. 766–776, 2006. doi: 10.1016/j.jsv.2005.12.004.

[37] L. Walls, "*Test Rig Design for Simulation and Identification of Rail Corrugation,"* bachelor thesis, Faculty of Engineering, Physical Sciences and Architecture, The University of Queensland, Queensland, 2003.

[38] P.A. Meehan, X. Liu, "*Modelling and mitigation of wheel squeal noise amplitude,"* Journal of Sound and Vibration, vol. 413, pp. 144–158, 2018 doi: 10.1016/j.jsv.2017.10.032.

[39] P.A. Meehan, X. Liu, "*Modelling and mitigation of wheel squeal noise under friction modifiers,"* Journal of Sound and Vibration, vol. 440, pp. 147 – 160, 2019. doi: 10.1016/j.jsv.2018.10. 025.

[40] S. Liu, U. De Silva, D. Chen, A.C. Leslie, P.A. Meehan, "*Investigation of wheel squeal noise under mode coupling using two-disk testrig experiments,"* Wear, no. 205035, 2023. doi: 10.1016/j.wear.2023.205035.

[41] M. Omasta, V. Navrátil, T. Gabriel, R. Galas, M. Klapka, "*Design and Development of a Twin Disc Test Rig for the Study of Squeal Noise from the Wheel – Rail Interface,"* Applied Engineering Letters : Journal of Engineering and Applied Sciences, vol. 7, pp. 10–16, 2022. doi: 10.18485/aeletters.2022.7.1.2.

[42] E. Schneider, K. Popp, H. Irretier, "*Noise generation in railway wheels due to rail-wheel contact forces,"* Journal of Sound and Vibration, vol. 120, pp. 227–244, 1988. doi: 10.1016/ 0022-460X(88)90431-2.

[43] P.A. Meehan, "*Prediction of wheel squeal noise under mode coupling,"* Journal of Sound and Vibration, vol. 465, no. 115025, 2020. doi: 10.1016/j.jsv.2019.115025.

[44] Y.A. Areiza, S.I. Garcés, J.F. Santa, G. Vargas, A. Toro, "*Field measurement of coefficient of friction in rails using a hand-pushed tribometer,"* Tribology International, vol. 82, pp. 274–279, 2015. doi: 10.1016/j.triboint.2014 .08. 009.

[45] B. Ding, G. Squicciarini, D. Thompson, R. Corradi, "*An assessment of mode-coupling and falling-friction mechanisms in railway curve squeal through a simplified approach,"* Journal of Sound and Vibration, vol. 423, pp. 126–140, 2018. doi: 10.1016/j.jsv.2018.02.048.

[46] E.A. Gallardo-Hernandez, R. Lewis, "*Twin disc assessment of wheel/rail adhesion,"* Wear, vol. 265, pp. 1309–1316, 2008. doi: 10.1016/j. wear.2008.03.020.

[47] H. Chen, S. Fukagai, Y. Sone, T. Ban, A. Namura, *"Assessment of lubricant applied to wheel/rail interface in curves,"* Wear, vol. 314, pp. 228–235, 2014. doi: 10.1016/j.wear.2013. 12.006.

[48] Z.Y. Shen, J.K. Hedrick, J.A. Elkins, *"A Comparison of Alternative Creep Force Models for Rail Vehicle Dynamic Analysis,"* Vehicle System Dynamics, vol. 12, pp. 79–83, 1983. doi: 10.1080/00423118308968725.

[49] X. Liu, P.A. Meehan, "*Investigation of squeal noise under positive friction characteristics condition provided by friction modifiers,"* Journal of Sound and Vibration, vol. 371, pp. 393–405, 2016. doi: 10.1016/j.jsv.2016.02.028.

[50] R. Galas, M. Omasta, L. Shi, H. Ding, W. Wang, I. Krupka, M. Hartl, "*The low adhesion problem: The effect of environmental conditions on adhesion in rolling-sliding contact,"* Tribology International, vol. 151, no. 106521, 2020. doi: 10.1016/j.triboint.2020.106521.

[51] C. Hardwick, R. Lewis, U. Olofsson, "*Low adhesion due to oxide formation in the presence of salt*," Proceedings of the Institution of Mechanical Engineers, Part F: Journal of Rail and Rapid Transit, vol. 228, pp. 887–897, 2014. doi: 10.1177/0954409713495666.

[52] L.E. Buckley-Johnstone, G. Trummer, P. Voltr, A. Meierhofer, K. Six, D.I. Fletcher, R. Lewis, *"Assessing the impact of small amounts of water and iron oxides on adhesion in the wheel/rail interface using High Pressure Torsion testing,"* Tribology International, vol. 135, pp. 55–64, 2019. doi: 10.1016/j.triboint.2019.02. 024.

[53] R. Galas, M. Omasta, M. Klapka, S. Kaewunruen, I. Krupka, M. Hartl, "*Case study: The influence of oil-based friction modifier quantity on tram braking distance and noise*," Tribology in Industry, vol. 39, pp. 198–206, 2017. doi: 10.24874/ti.2017.39.02.06.

[54] L. Buckley-Johnstone, M. Harmon, R. Lewis, C. Hardwick, R. Stock, "*A comparison of friction modifier performance using two laboratory test scales*," Proceedings of the Institution of Mechanical Engineers, Part F: Journal of Rail and Rapid Transit, vol. 233, pp. 201–210, 2019. doi: 10.1177/0954409718787045

[55] R. Galas, M. Omasta, I. Krupka, M. Hartl, "*Laboratory investigation of ability of oil-based friction modifiers to control adhesion at wheel-rail interface*," Wear, vol. 368–369, pp. 230–238, 2016. doi: 10.1016/j.wear.2016. 09.015.

[56] D. Kvarda, S. Skurka, R. Galas, M. Omasta, L. Shi, H. Ding, W. Wang, I. Krupka, M. Hartl, "*The effect of top of rail lubricant composition on adhesion and rheological behaviour*," Engineering Science and Technology, an International Journal, vol. 35, no. 101100, 2022. doi: 10.1016/j.jestch.2022.101100.

[57] R. Galas, S. Skurka, M. Valena, D. Kvarda, M. Omasta, H. Ding, Q. Lin, W. Wang, I. Krupka, M. Hartl, "*A benchmarking methodology for top-of-rail products*," Tribology International, vol. 189, no. 108910, 2023. doi: 10.1016/j.trboint.2023.108910.

[58] S. Skurka, R. Galas, M. Omasta, B. Wu, H. Ding, W.-J. Wang, I. Krupka, M. Hartl, "*The performance of top-of-rail products under water contamination*," Tribology International, vol. 188, no. 108872, 2023. doi: 10.1016/j.trboint.2023. 108872.

[59] M. Moreno-Ríos, E.A. Gallardo-Hernández, M. Vite-Torres, A. Peña-Bautista, "*Field and laboratory assessments of the friction coefficient at a railhead*," Proceedings of the Institution of Mechanical Engineers, Part F: Journal of Rail and Rapid Transit, vol. 230, pp. 313–320, 2016. doi: 10.1177/0954409714536383

Supplementary material

Table A1 – traction curves – Measured lateral adhesion coefficient.

Angle of attack (mrad)	**2,5**	**5**	**10**	**15**	**20**	**25**	**30**	**35**
μ (1) - 2 m/s - DRY	0.2634	0.4429	0.5036	0.4869	0.4544	0.4434	0.4552	0.4332
σ (1)	0.0423	0.0142	0.0383	0.0214	0.0300	0.0197	0.0251	0.0291
μ (1) - 4 m/s - DRY	0.2457	0.4404	0.4588	0.4837	0.4745	0.4658	0.4367	0.4025
σ (1)	0.0529	0.0249	0.0176	0.0183	0.0342	0.0201	0.0218	0.0290
μ (1) - 2 m/s - WET	0.2739	0.3642	0.3736	0.3695	0.3680	0.3595	0.3966	0.3652
σ (1)	0.0153	0.0304	0.0240	0.0264	0.0436	0.0305	0.0154	0.0250
μ (1) - 4 m/s - WET	0.2534	0.3572	0.3618	0.3318	0.3335	0.3531	0.3388	0.3558
σ (1)	0.0318	0.0247	0.0386	0.0351	0.0259	0.0372	0.0184	0.0282

Table A2 – Sound pressure levels during tests under dry and wet conditions.

Angle of attack (mrad)	**2,5**	**5**	**10**	**15**	**20**	**25**	**30**	**35**
SPL (dB) - 2 m/s - DRY	77.5	86.8	100.6	100.5	102.4	104.3	105.5	106.1
σ (dB)	0.5	1.2	0.9	0.7	0.4	0.6	0.5	0.7
SPL (dB) - 4 m/s - DRY	85.6	98.0	102.8	104.7	106.1	106.9	107.5	107.9
σ (dB)	0.3	2.1	1.7	0.8	0.6	0.5	0.3	0.6
SPL (dB) - 2 m/s - WET	75.2	82.8	84.6	89.1	89.9	88.9	89.0	89.5
σ (dB)	0.4	0.9	0.6	1.5	1.1	0.4	0.9	0.6
SPL (dB) - 4 m/s - WET	83.5	90.8	91.4	97.9	97.4	97.7	96.3	97.2
σ (dB)	0.3	0.6	0.9	1.1	1.2	0.9	1.5	1.1

Table A3 – Vibration velocities during tests under dry and wet conditions at 445 Hz.

Angle of attack (mrad)	**2,5**	**5**	**10**	**15**	**20**	**25**	**30**	**35**
$\dot{y}$ (mm/s) - 2 m/s - DRY	0.20	0.30	0.72	2.87	5.71	5.97	6.10	6.35
σ (mm/s)	0.06	0.05	0.12	0.20	0.27	0.47	0.34	0.41
$\dot{y}$ (mm/s) - 4 m/s - DRY	0.48	0.57	3.77	4.34	4.47	5.14	5.08	5.20
σ (mm/s)	0.07	0.08	0.53	0.39	0.22	0.36	0.56	0.38
$\dot{y}$ (mm/s) - 2 m/s - WET	0.18	0.43	0.77	1.61	2.08	2.70	2.97	3.15
σ (mm/s)	0.04	0.06	0.12	0.16	0.15	0.20	0.26	0.31
$\dot{y}$ (mm/s) - 4 m/s - WET	0.32	0.80	0.93	1.19	1.24	1.28	1.64	1.93
σ (mm/s)	0.05	0.19	0.13	0.11	0.15	0.12	0.21	0.22

Table A4 – Vibration velocities during tests under dry and wet conditions at 1087 Hz.

Angle of attack (mrad)	**2,5**	**5**	**10**	**15**	**20**	**25**	**30**	**35**
$\dot{y}$ (mm/s) - 2 m/s - DRY	/	/	0.84	1.07	1.77	2.71	3.11	3.33
σ (mm/s)	/	/	0.13	0.11	0.25	0.33	0.19	0.25
$\dot{y}$ (mm/s) - 4 m/s - DRY	/	0.89	1.71	3.54	8.65	11.05	12.11	12.52
σ (mm/s)	/	0.11	0.38	0.33	0.62	1.23	1.52	1.34
$\dot{y}$ (mm/s) - 2 m/s - WET	/	0.22	0.67	0.87	0.76	0.82	1.07	1.18
σ (mm/s)	/	0.05	0.10	0.24	0.11	0.09	0.11	0.10
$\dot{y}$ (mm/s) - 4 m/s - WET	/	0.68	1.45	1.88	1.94	2.80	3.92	4.21
σ (mm/s)	/	0.11	0.20	0.33	0.25	0.23	0.44	0.38

Table A5 – Vibration velocities during tests under dry and wet conditions at 1923 Hz.

Angle of attack (mrad)	**2,5**	**5**	**10**	**15**	**20**	**25**	**30**	**35**
$\dot{y}$ (mm/s) - 2 m/s - DRY	/	/	0.63	0.82	3.55	3.78	4.45	4.72
σ (mm/s)	/	/	0.09	0.19	0.33	0.46	0.68	0.56
$\dot{y}$ (mm/s) - 4 m/s - DRY	/	0.30	1.58	2.50	2.44	3.37	3.70	4.12
σ (mm/s)	/	0.09	0.41	0.21	0.41	0.38	0.22	0.44
$\dot{y}$ (mm/s) - 2 m/s - WET	/	/	/	/	/	/	/	/
σ (mm/s)	/	/	/	/	/	/	/	/
$\dot{y}$ (mm/s) - 4 m/s - WET	/	/	0.24	0.25	0.27	0.28	0.22	0.29
σ (mm/s)	/	/	0.04	0.04	0.06	0.05	0.06	0.04

Table A6 – Results of experiments with different water amounts.

Amount (ml)	**1**	**2**	**5**	**10**
$\Delta\mu$ (1)	0.07	0.07	0.09	0.06
σ (1)	0.02	0.01	0.01	0.01
ΔSPL (dB)	11.2	10.5	10.5	9.2
σ (dB)	0.2	0.2	0.2	1.0
Δt (s)	156	297	618	917
σ (s)	28	18	15	17